An Integrated MEMS System for Turbulent Boundary Layer Control

Thomas Tsao*, Fukang Jiang*, Raanan Miller*, Yu-Chong Tai*,
Bhusan Gupta*, Rodney Goodman*, Steve Tung**, and Chih-Ming Ho**
*MS 136-93 California Institute of Technology
Pasadena, CA 91125, USA, tomster@touch.caltech.edu
**Mechanical and Aerospace Engineering Dept.,
University of California, Los Angeles
Los Angeles, CA, USA

SUMMARY

The goal of this project is a first attempt to achieve active drag reduction using a large-scale integrated MEMS system. Previously, we have reported the successful development of a shear-stress imager which allows us to "see" surface vortices [1]. Here we present the promising results of the interaction between micro flap actuators and vortices. It is found that microactuators can actually reduce drag to values even lower than the drag associated with pure laminar flow, and that the microactuators can reduce shear stress values in turbulent flow as well. Based on these results, we have attempted the first totally integrated system that consists of 18 shear stress sensors, 3 magnetic flap-type actuators and control electronics for use in turbulent boundary layer control studies.

Keywords: Integration, Flow Control

INTRODUCTION

For turbulent fluid flow across a surface, there exist structures of counter rotating vortices similar to those shown in Fig 3. These vortices bring high momentum fluid down to the surface, increasing surface shear stress. Integrated over a surface, this shear stress leads to the total surface drag. At Reynolds numbers of 10^5 (which corresponds to airplane flight), the lifetime of these structures is on the order of milliseconds, and the size is on the order of millimeters. In addition, these structures appear randomly in time and space. The parameters of this problem suggest a spatially distributed sensor and actuator system as a necessary way to reduce drag. We envision a fully integrated real-time MEMS system in which the shear stress sensors detect the vortices, the electronics process the sensor signal, and the actuators weaken, if not terminate, the vortices. Such a distributed system would require, over a standard 100 mm wafer, thousands of millimeter sized actuators and tens of thousands of sub-millimeter sized sensors all connected by integrated circuitry. This system would then maintain a laminar flow at a high Reynolds number (>2000) when turbulence normally occurs.

Our group has reported the successful development of shear stress imagers [1] which allow us to detect and even "see" turbulent vortices. Here, discussion is on actuators, the interaction between actuators and vortices, and the total system integration.

ACTUATOR-FLOW INTERACTION

First, we report here the feasibility study of using torsional microactuators to reduce the shear stress under a turbulent streak. We have conducted two sets of wind tunnel experiments. Both used bulk micromachined magnetic flap-type actuators [2]. Fig 1 shows a schematic representation of the wind tunnel test set-up.

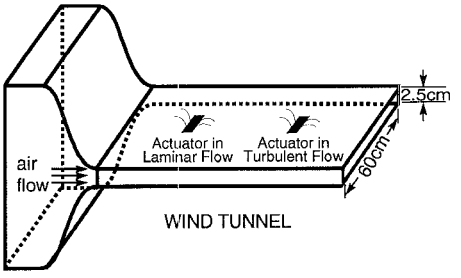

Fig 1. Schematic representation of the wind tunnel testing set-up. Upstream, the flow is laminar and needs a vortex generator to create a stationary vortex for the actuator to interact with. Downstream, the flow is naturally turbulent.

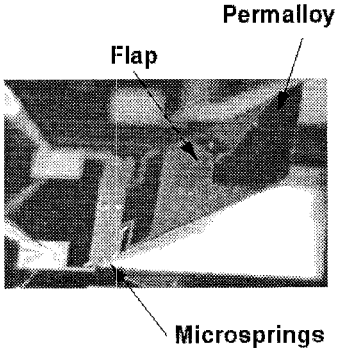

Fig 2. Example of a bulk micromachined flap used in one of the actuator-flow interaction experiments in laminar flow. The flap is 4x4 mm^2.

The first set of experiments was designed to measure actuator-flow interaction in a laminar flow. Because there are no short-lived turbulent structures in this flow, the relatively large (4x4 mm^2) actuators (Fig 2) used were designed to

provide large displacements, typically 1 or 2 mm, at low frequencies, typically less than 100 Hz. In these experiments, we first perturbed the laminar flow with a vortex generator. (Fig 3 (a).) Actuators [2,3] were activated downstream in the turbulent flow, and hot-wire sensors were then placed after the actuators to determine the effect of the actuation. Hot wire sensors, instead of shear stress sensors, were used because the large width of the actuator resulted in the actuator-flow interaction having an effect over a width of over 5 cm. The hot wire sensors were used to measure the velocity flow field, from which velocity gradients, and hence shear stress, drag force, and drag coefficient can be derived. The results are shown in Fig 4 where drag coefficient is plotted against the phase of an actuator at different frequencies.

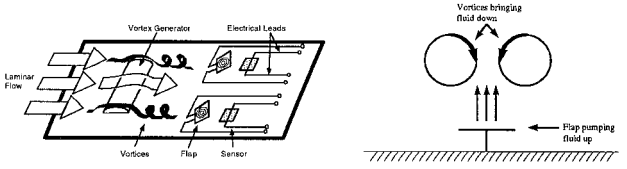

(a) (b)

Fig 3. (a) Schematic of vortex generator set-up (b) Cross section of vortex-actuator interaction.

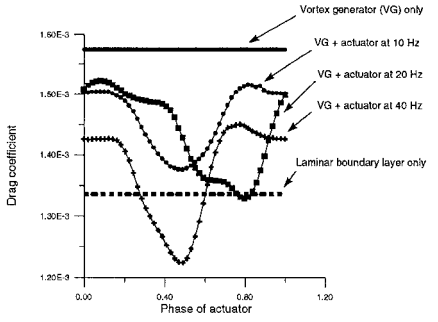

Fig 4. Graph showing drag coefficient as a function of actuator phase. A vortex generator is used to induce a stationary vortex in an otherwise laminar flow. At 40 Hz, the drag coefficient is actually lower than if the flow were laminar. Drag coefficient (C_d) is defined as drag force/dynamic (or wind loading) force.

The proposed mechanism (Fig 3 (b).) for reducing shear stress is that the microactuator provides the upwards "pumping" of fluid to counteract the effect of the vortices so that high momentum fluid is blown away from the surface. In Fig 4, the results show the first promising evidence that the magnetic actuator can be used to reduce drag. In fact, under certain conditions, the drag coefficient across a test surface was even lower than the drag coefficient on the same surface under laminar flow conditions. In addition, work has also been done (Fig 5) that suggests that ωA (angular frequency multiplied by flap deflection, or tip velocity) may be the important control parameter.

The first set of experiments provided the proof-of-concept for the idea that micro-actuators can be used to affect boundary layer flow. The next step was to design a set of experiments to test micro-actuator/flow interaction in fully

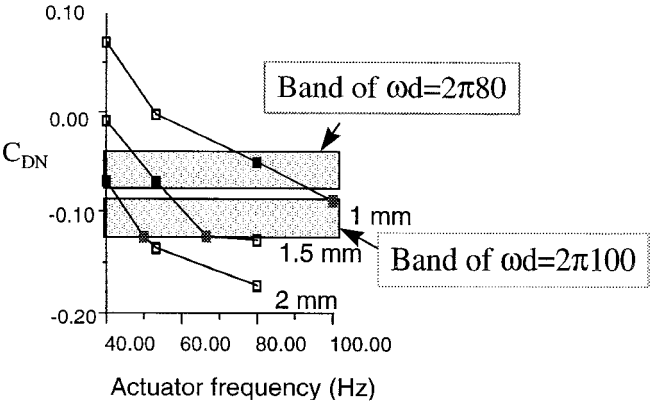

Fig. 5. Graph showing (for different amplitudes) drag reduction/increase as a function of frequency. C_{DN} is defined as $(C_d-C_{dl})/C_{dl}$ where C_{dl} is the drag coefficient in a laminar flow. A negative value on the y-axis represents drag reduction. Each curve represents a different amplitude (measured in mm) actuation. Different points with the same value of ωA have approximately the same drag reduction effect.

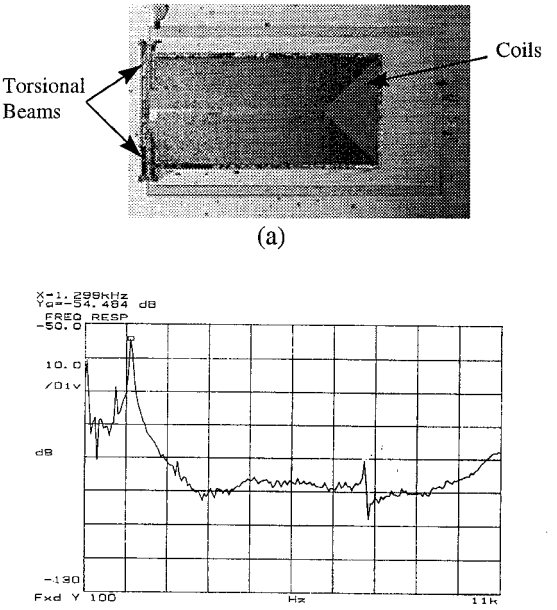

Fig 6. (a) Picture of magnetic flap used in actuator-flow interaction testing in fully developed turbulent flow. The flap is 2x1 mm². (b) Frequency response of actuator shown in (a). The first order resonant frequency is 1.3 kHz. The higher resonance (7.45 kHz) corresponds to a twisting mode.

developed turbulent flow. The parameters of this experiment, in particular the millisecond life-time of vortices at high Reynolds number, require that we design an actuator capable of high frequency operation. Due to the inherent tradeoff between high frequency operation and large displacement actuation, these actuators were operated at their resonant frequency to obtain maximum ωA. Given the width of the

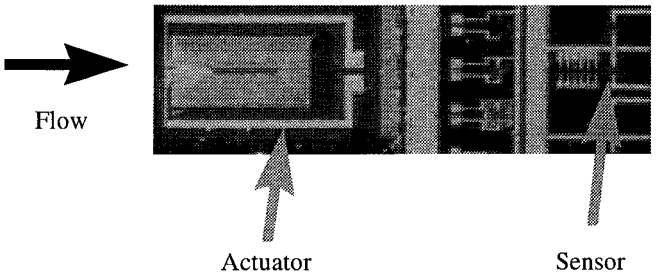

Fig 7. Picture showing actuator and sensor package used to study actuator/flow interaction in fully developed turbulent flow.

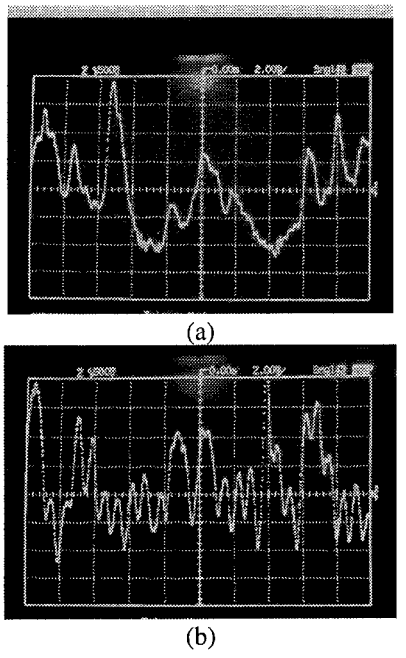

Fig 8. (a) Oscilloscope display of a shear stress sensor output in a fully developed turbulent flow with a mean flow of 10 m/s. The time scale is 2 ms/div and the voltage scale is 500 mV/div. This is a typical shear stress sensor output [4].(b) Similar to (a) but with actuation at 1.3 kHz (resonant frequency of actuator). A 1.3 kHz signal is clearly seen in the output, indicating that the actuation is affecting the flow in a significant manner.

vortices, we have designed narrower actuators (2.5 mm long by 1 mm wide). Fig. 6(a) shows an example of such an actuator and Fig. 6 (b) shows its frequency response.

In the experimental set-up, we wire-bonded an actuator chip (upstream) and a shear stress sensor chip (downstream) next to each other on a small PC board (Fig 7) and placed the board in the fully developed turbulent flow portion of the wind tunnel. We then measured the shear stress output from a single sensor under various conditions.

Fig 8 (a) shows an oscilloscope trace of the shear stress sensor output when there is no actuation. This is representative of a typical shear stress sensor output [5]. When the actuator is activated at its resonant frequency (1.3 kHz, displacement approximately 100 μm), a typical shear stress sensor output is shown in Fig 8 (b). A 1.3 kHz signal is clearly visible. This shows that the actuator affects the turbulent flow to a significant degree. When there is actuation, but no flow, the shear stress sensor output registers nothing. This indicates two things: first, that there is no cross talk between the sensor and actuator, and second, that the actuator by itself does not produce a disturbance large enough to be sensed; the perturbations must be carried downstream by the mean flow.

All of this work was done using a hybrid approach where the components were on different substrates and wire-bonded to each other. As it is shown that a single actuator can reduce the drag caused by a vortex (Fig 4), we can then proceed to make an integrated system to show that collectively, thousands of sensors and actuators can also reduce drag over a large area. We have then pursued the difficult task of overall system integration, the first step of which is to integrate sensors, actuators, and electronics all on the same chip.

INTEGRATION TECHNOLOGY

We have developed a technology to integrate the shear stress sensors, microactuators, and CMOS circuitry together to implement our total system. Several wafers have been processed and each prototype chip (Fig. 9) consists of electronics and two rows of sensors sandwiching a row of actuators. As turbulent air flows past the first row of sensors, the circuitry [5] will detect regions of high shear stress and send a signal to actuate the flap. The row of sensors after the actuator will then be used to determine the effect of the actuation on shear stress.

Using this chip in conjunction with a flexible off-chip actuator control waveform, we will be able to determine the best control algorithm. We have designed chips which use both surface and bulk micromachined actuators. All work done on integrating MEMS with electronics has a primary concern: the order in which the electronics and MEMS components are fabricated. We have chosen a hybrid approach (Fig. 11) where electronics up to metal is fabricated at an outside foundry such as UC-Berkeley's microlab. All of the high temperature MEMS steps (i.e. LPCVD polysilicon and nitride depositions) are then done in our lab. Electronics metallization is then completed at Berkeley. Finally, we finish the low temperature MEMS steps, including sacrificial layer etching for the surface micromachined actuators.

The integration process is far more complex than the sum of the individual processes. Many steps are included as protection masks, which serve to protect the parts of the system not being processed at the time. Lithography can be a problem, as relatively thick photoresist (approximately 4 μm) must be used for step coverage near the end of the process. This can be troublesome when patterning small contact holes or fine metal lines for the electronics. Many other steps are included to increase the yield of the overall process. Totally, the process includes 22 masking steps. Another concern when doing integration is the sacrificial layer etching for the surface micromachined flaps. Oxide cannot be used as a sacrificial

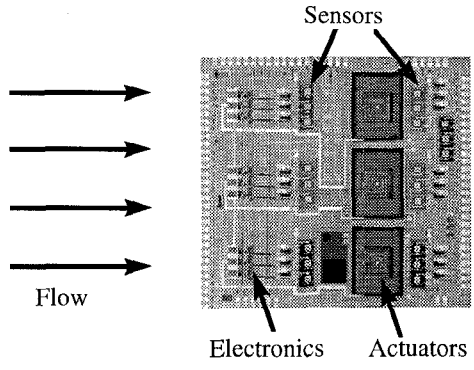

Fig. 9. Picture showing a 1x1 cm^2 die with shear stress sensors, actuators, and electronics. The surface micromachined actuators were freed in BrF_3.

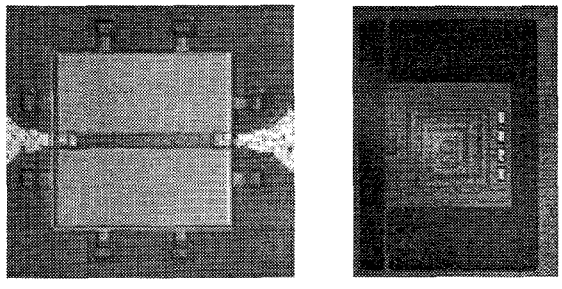

Fig. 10. Examples of shear stress sensor (left) and surface micromachined actuator used in the integration process. The sensor is 250x250 μm^2. The actuator plate is 1x1 mm^2.

layer because it is also the circuit encapsulation material. We have therefore chosen polysilicon as the sacrificial layer and have released the actuators using both TMAH and BrF_3, a gas phase release agent whose properties are presented in a separate paper in these conference proceedings. The dry release is important for eliminating stiction, which is a big problem because a high yield of actuators is needed across an entire wafer.

A picture of an integrated die with surface micromachined flaps is shown in Fig 9. The flaps were released with BrF_3. Unfortunately, the electronics yield in the process used to fabricate our system was too low so we cannot produce system-level testing results at this moment.

FUTURE WORK

We will continue to test different high frequency actuators to help determine an ideal control mechanism for drag reduction. Until we have a single integrated chip, we will conduct experiments by wire-bonding the various discrete components together. Meanwhile, we will continue to work with outside vendors to improve the yield of the electronics so that we can achieve our ultimate goal of a single chip solution.

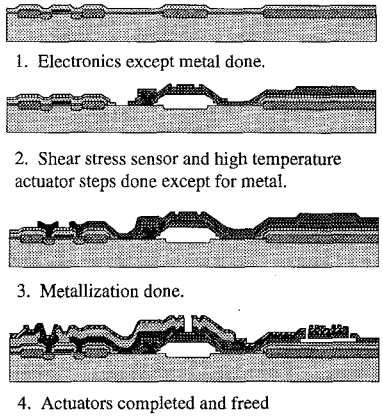

Fig. 11. Drawing showing simplified process flow. Steps 1 and 3 are completed at a vendor (in the case of Fig 10, UC-Berkeley), while 2 and 4 are completed at CalTech.

CONCLUSIONS

We have demonstrated the feasibility of controlling turbulent structures using low and high frequency magnetic actuators. We have designed a system and developed an integration technology to fabricate a prototype system for turbulent boundary layer control.

ACKNOWLEDGEMENTS

This work is sponsored by the AFOSR University Research Initiative (URI) program under grant #F49620-93-1-0332.

REFERENCES

[1] F. Jiang, Y.-C. Tai, B. Gupta, and R. Goodman, "A Surface Micromachined Shear Stress Imager," MEMS '96, pp 110-115. 1996.

[2] R. Miller, Y.-C. Tai, G. Burr, D. Psaltis, C.-M. Ho, and R. Katti, "Electromagnetic MEMS Scanning Mirrors for Holographic Data Storage", Solid State Sensor and Actuator Workshop 1996, pp 183-186, 1996.

[3] T. Tsao, C. Liu, and Y.-C. Tai, "Micromachined Magnetic Actuator for Active Fluid Control," ASME Application of Microfabrication to Fluid Mechanics 1994, pp 31-38. 1994.

[4] C. Liu, T. Tsao, Y.-C. Tai, "Micromachined Permalloy Magnetic Actuator for Delta-Wing Control," MEMS '95, pp 332-335, 1995.

[5] C. Liu, Y.-C. Tai, J.-B. Huang, and C.-M. Ho, "A Silicon Micromachined Thermal Shear Stress Sensor", ASME Application of Microfabrication to Fluid Mechanics 1994, pp 9-15, 1994.

[6] B. Gupta, *Analog VLSI for Active Drag Reduction*, Ph.D. Thesis, California Institute of Technology, 1997.